

Optical, photoluminescent, and photoconductive properties of functionalized anthradithiophene and benzothiophene derivatives

Whitney E.B. Shepherd^a, Andrew D. Platt^a, Garrett Banton^a, Marsha A. Loth^b, John E. Anthony^b and Oksana Ostroverkhova^a

^aDepartment of Physics, Oregon State University, Corvallis, OR 97331, USA;

^bDepartment of Chemistry, University of Kentucky, Lexington, KY 40506, USA

ABSTRACT

We present optical, photoluminescent (PL), and photoconductive properties of functionalized anthradithiophene (ADT) and benzothiophene (BTBTB) derivatives and their composites. Solution-deposited ADT films exhibit charge carrier mobilities of over 1.5 cm²/Vs, high PL quantum yields, and high photoconductivity at room temperature. We show molecular arrangement and intermolecular interactions significantly contribute to the (opto)electronic properties of thin films of these pi-stacked materials. In addition, these properties can be effectively manipulated through the addition of guest molecules to a host material. In particular, exciton and charge carrier dynamics can be varied using a competition between photoinduced charge and energy transfer in a guest-host system. To better understand these processes at a molecular level, we apply single-molecule fluorescence spectroscopy (SMFS) to probe the effects of intermolecular interactions on the molecular properties. Specifically, we demonstrate that ADT molecules exhibit high enough quantum yields and photostability to be imaged on a single-molecule level at room temperature. Moreover, we show that stability of single ADT molecules immobilized in a solid-state matrix are comparable to those of the best fluorophores utilized in SMFS.

Keywords: Organic Semiconductors, Photoconductivity, Single Molecule Fluorescence Spectroscopy

1. INTRODUCTION

Organic semiconductor materials have garnered a lot of interest due to their low-cost, tunable properties and potential applications in optical and electronic devices.¹ Several solution-processable functionalized anthradithiophene (ADT) derivatives have been synthesized which exhibit charge carrier (hole) mobilities of over 1.5 cm²/Vs in spin-coated thin films,²⁻⁴ fast charge carrier photogeneration, and high continuous wave (cw) photoconductivity.^{5,6} Availability of various solution-processable derivatives also enabled investigations of charge and energy transfer processes and their contribution to photoconductive and photoluminescent (PL) properties of composites of these materials.⁷ For example, combinations of two ADT derivatives, ADT-TIPS-CN and ADT-TES-F, have been shown to exhibit strong energy transfer in solid state, leading to considerably different charge carrier dynamics in thin films of this composite, as compared to those in pristine films.^{7,8} Furthermore, ADT derivatives exhibit high PL quantum yields and photostability, and can be imaged on a single molecule level,⁹ which opens up possibilities to study charge and energy transfer processes on a molecular level in these technologically important materials.

In this paper, we explore novel combinations of solution-processable functionalized ADT and benzothiophene (BTBTB) derivatives and their optical, PL, and photoconductive properties. In addition to bulk properties, we investigate properties of ADT molecules as single-molecule fluorescent reporters in a solid-state environment, with a future goal of establishing the feasibility of using ADT/BTBTB composites for studies of charge and energy transfer processes on a single-molecule level.

Further author information: (Send correspondence to O.O.)

O.O.: E-mail: oksana@science.oregonstate.edu, Telephone: 1 541 737 1679

J.E.A.: E-mail: anthony@uky.edu, Telephone: 1 859 257 8844

2. EXPERIMENTAL

2.1 Materials and Sample Preparation

We studied thin films of a benzothiophene derivative functionalized with (t-butyl)ethynyl side groups, 6,12-bis[2-(t-butyl)ethynyl]-Benzo[1,2-b:4,5-b']bis[1]benzothiophene (t-bu BTBTB), both pristine and with the addition of small amounts of an ADT derivative, both shown in Figure 1. The fluorinated ADT derivative under study, ADT-TES-F, is functionalized with triethylsilylethynyl (TES) side groups. Synthesis and characterization of optical and electronic properties of ADT-TES-F have been reported elsewhere.^{3,5} Functionalized benzothiophenes are a newer class of materials, and synthesis of t-bu BTBTB will be reported in a subsequent paper. The highest occupied and lowest unoccupied molecular orbital (HOMO and LUMO) energies of ADT-TES-F (t-bu BTBTB) were measured in solution using differential pulse voltammetry⁵ and yielded 5.35 (5.75) eV and 3.05 (2.23) eV for the HOMO and LUMO levels, respectively.

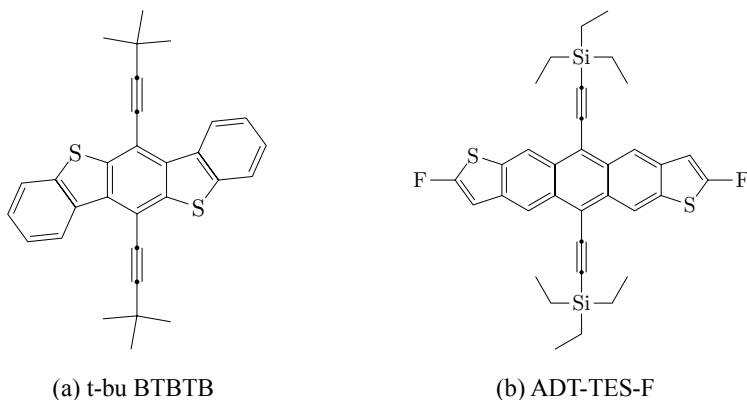


Figure 1. Molecular structures of (a) t-bu BTBTB and (b) ADT-TES-F derivatives.

Stock solutions of t-bu BTBTB were prepared at 10^{-2} M in chlorobenzene. For bulk studies, the ADT-TES-F was then added at ratios of 2 mol %, 0.2 mol %, and 0.02 mol % to t-bu BTBTB. For (photo)conductivity and bulk fluorescence measurements, solutions were drop cast onto glass substrates at 65 °C to make polycrystalline films of 1-2 μm in thickness. The glass substrates used for dark and photoconductivity measurements contained photolithographically deposited 5 nm/50 nm thick Cr/Au electrode pairs. Each pair consisted of 10 interdigitated finger pairs, with 1 mm finger length, 25 μm finger width and 25 μm gaps between the fingers of opposite electrodes.

Samples for photobleaching quantum yield (Φ_b) measurements were prepared in 0.5% polymethylmethacrylate (PMMA) by weight in toluene at a ratio of 0.2 mol % of fluorophore in PMMA. Films were then spin coated as described below. Photobleaching quantum yield in t-bu BTBTB was measured in 0.2 mol % of fluorophore in t-bu BTBTB drop cast films.

For single molecule fluorescence spectroscopy (SMFS), samples were prepared in 1 wt % solution of PMMA (75,000 m.w., Polysciences, Inc.) in toluene at a concentration of 10^{-10} mol/mol of the fluorophore (ADT-TES-F) to PMMA. The glass coverslips were cleaned by first sonicating them for 20 minutes in a detergent bath. They were then rinsed in deionized (DI) water and placed in a 50% sulfuric acid bath which was heated to $\sim 60^\circ\text{C}$ for one hour. After the acid soak, they were rinsed in DI water followed by a rinse in ultrapure DI water (18.2 M Ω). Finally, the substrates were dried under an N₂ stream. The samples were prepared by spin coating of the solution onto cleaned glass coverslips at 2000 rpm for 55 s.

2.2 Optical Properties

PL emission spectra were acquired in a custom PL measurement setup with laser excitation at wavelengths of either 355 nm (cavity Q- switched Nd:YVO₄ at 44.6 kHz from Nanolase) or cw 532 nm (Nd:YVO₄ from Coherent,

Inc.). Emitted photons were collected using a parabolic mirror and detected with a fiber coupled spectrometer (Ocean Optics USB2000) calibrated against a 3100 K black-body emitter.

PL lifetimes were measured under 400 nm, 80 fs pulsed excitation generated from a frequency doubled (with a beta-barium borate crystal) mode-locked Ti:Sapphire laser. The mode-locked repetition rate is 93.3 MHz which is picked at 9.3 MHz using a custom built pulse picker based on a TeO₂ acousto-optic modulator from NEOS. A single-photon avalanche photodiode (SPAD, Molecular Photonic Devices) was used in conjunction with a time-correlated single-photon counter (TCSPC) data analysis board (PicoQuant TimeHarp 200) for detection. The instrument response function (IRF \sim 200 ps) was recorded using scattered light from an etched microscope slide.

2.3 Dark Current and Dc Photocurrent Measurements

For dark current and dc photocurrent measurements, a Keithley 237 source-measure unit was used to measure current through the sample in the absence and in the presence of a 532 nm cw or 355 nm pulsed (time-averaged) photoexcitation incident on from the substrate side. The photocurrent was calculated as the difference between the two. Light intensity was \sim 15 mW/cm² for both 532 nm and 355 nm measurements.

2.4 Photobleaching Quantum Yield

Photobleaching quantum yield was calculated according to Eq.1, where n_{bleach} is the number of molecules bleached, N_{phot} is the number of photons absorbed, R_{phot} is the photon absorption rate, σ_λ and I_λ are the absorption cross section and intensity at the excitation wavelength (λ), respectively. The time constant τ_b was determined by fitting the photobleaching dynamics of different fluorophores with a bi-exponential function. A weighted average was then taken of the fitted time constants to arrive at τ_b .¹⁰

$$\Phi_b = \frac{n_{bleach}}{N_{phot}} = \frac{1}{\tau_b R_{phot}} = \frac{1}{\tau_b \sigma_\lambda I_\lambda \left(\frac{\lambda}{hc}\right)} \quad (1)$$

A bulk estimate of N_{tot} , the average total photons emitted by a single fluorophore, can be calculated from the inverse of Φ_b as in Eq. 2, where Φ_F is the PL quantum yield.¹⁰

$$N_{tot} = \frac{\Phi_F}{\Phi_b} \quad (2)$$

2.5 Single Molecule Spectroscopy

Measurements of ADT-TES-F fluorescence on a single-molecule level were carried out under cw 532 nm (Nd:YVO₄ from Coherent, Inc.) wide-field illumination on an Olympus IX-71 inverted microscope with a 100X UPlanApo (NA 1.4) objective. Fluorescence was imaged with an Andor iXon EMCCD (DU-897) camera. Collection efficiency of the setup was determined according to $\eta = \eta_Q T_{ang} T_{opt} T_{filt}$, where T_{ang} is the angular collection factor, T_{opt} is the collection factor through the microscope optics, T_{filt} is the transmission through the filter and η_Q is the quantum efficiency of our camera.¹⁰ The collection efficiency, along with the A-to-D counts per electron sensitivity and electron multiplying gain settings were used to determine the number of emitted photons from the measured number of counts.

Image and video analysis were carried out using custom written Matlab scripts which locate the fluorophores and generate fluorescent trajectories. These were then used to create intensity histograms, and systems showing two-level behavior were selected. On and off times were calculated based on the threshold intensity determined from the intensity histogram.^{11,12}

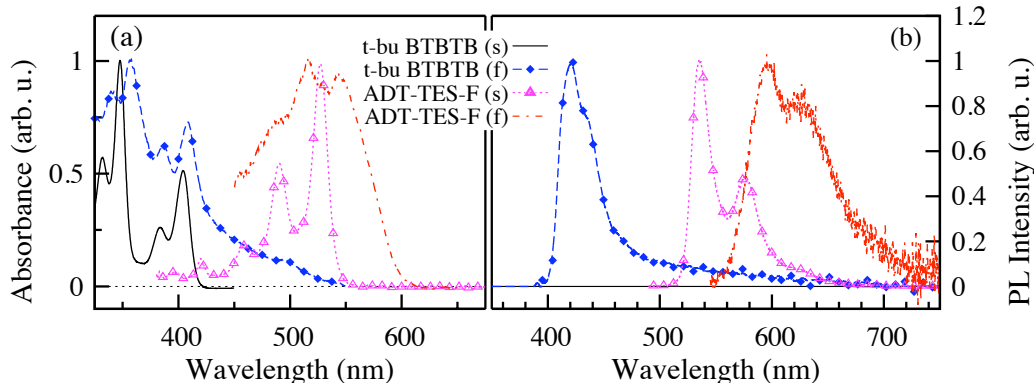


Figure 2. (a) Absorption and (b) PL spectra of films and solutions of pristine t-bu BTBTB and ADT-TES-F at 355 nm and 532 nm excitation respectively.

3. RESULTS AND DISCUSSION

3.1 Optical Properties in Film

Figure 2 shows absorption and PL spectra of pristine t-bu BTBTB and ADT-TES-F (at 355 nm and 532 nm excitation, respectively) in solution and in film. No PL response was observed from t-bu BTBTB film at 532 nm excitation. Both compounds exhibited similar spectral features such as vibronic progression, solid-state red-shift, and broadening of the spectra (as compared to those in solution) due to exciton delocalization and intermolecular interaction.^{5,13}

In film, upon the addition of ADT-TES-F to t-bu BTBTB, the PL contribution from ADT-TES-F molecules was apparent and well separated spectrally from that of t-bu BTBTB under 355 nm illumination, as shown in Fig. 3. The emission spectra due to ADT-TES-F in t-bu BTBTB were only slightly red-shifted and broadened with respect to the ADT-TES-F spectra in solution, suggesting that at ADT-TES-F concentrations of 2 mol % and below, the degree of intermolecular interaction among ADT-TES-F molecules is significantly reduced (compared to pristine ADT-TES-F films in Fig. 2) and the ADT-TES-F is mostly behaving as isolated molecules in the t-bu BTBTB host. PL spectra at 355 nm excitation of the ADT-TES-F/t-bu BTBTB films also show quenching of the t-bu BTBTB PL with increasing ADT-TES-F concentration, indicative of energy transfer occurring from t-bu BTBTB to ADT-TES-F.^{7,14}

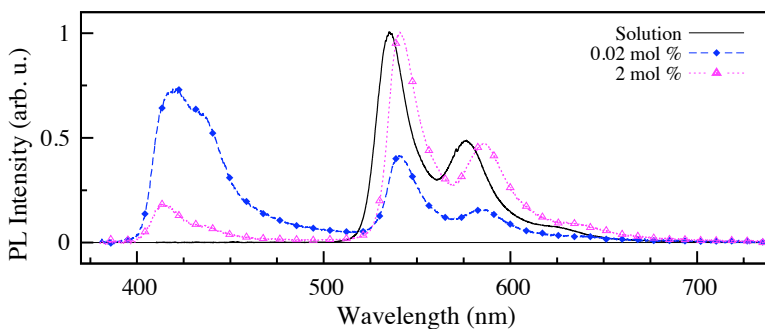


Figure 3. Spectra of ADT-TES-F/t-bu BTBTB films at two concentrations (2 mol % and .02 mol %) under 355 nm excitation. Solution spectrum of ADT-TES-F under 532 nm excitation is also shown.

Figure 4 shows PL decays measured in ADT-TES-F solution and ADT-TES-F and t-bu BTBTB pristine films. Also shown are the PL decay dynamics of the guest ADT-TES-F molecules in ADT-TES-F/t-bu BTBTB film (at 0.02 mol % ADT-TES-F concentration). While PL decays in solutions are single-exponential,⁵ those in films are better described by a bi-exponential function, $A_1 \exp[-t/\tau_1] + A_2 \exp[-t/\tau_2]$ where τ_1 and τ_2 are shorter and longer lifetimes and A_1 and A_2 are their relative amplitudes ($A_1 + A_2 = 1$), respectively.

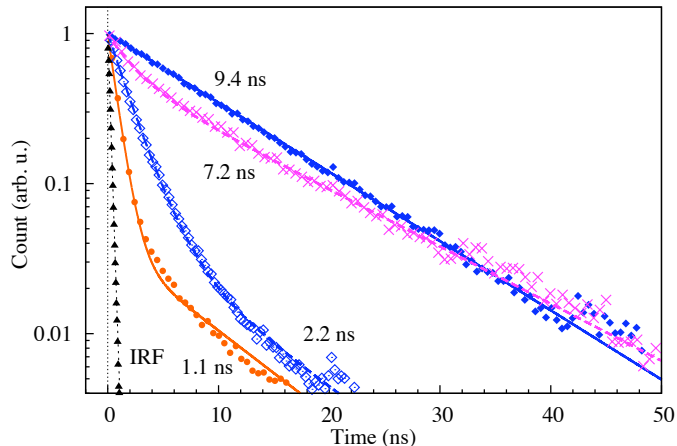


Figure 4. Normalized PL decays measured in solution of ADT-TES-F (◆), fitted with a single-exponential function. Also shown are PL decay dynamics obtained in polycrystalline films of ADT-TES-F (◇) and t-bu BTBTB (○). The films data are fitted with a bi-exponential function which yield averaged lifetimes of 2.2 ns and 1.1 ns for ADT-TES-F and t-bu BTBTB films, respectively. Also shown is the data obtained from the ADT-TES-F/t-bu BTBTB film at 0.02 mol % of ADT-TES-F fitted with a bi-exponential function with τ_{avg} of 7.2 ns (×). The instrument response function (IRF) (▲), with the full-width at half-maximum of ~ 200 ps is also included.

The PL decays measured in the ADT-TES-F/t-bu BTBTB films, characterized by an average time constant of 6.8-7.2 ns (calculated as a weighted average of τ_1 and τ_2 , $\tau_{ave} = A_1\tau_1 + A_2\tau_2$), were similar to that measured in ADT-TES-F in dilute solution (9.4 ns). This supports our earlier observation that at low concentration of ADT-TES-F in t-bu BTBTB, there is very weak intermolecular interaction between ADT-TES-F molecules, and there is no significant non-radiative relaxation due to interactions between ADT-TES-F and t-bu BTBTB molecules. In contrast, pristine ADT-TES-F (t-bu BTBTB) films exhibited an average lifetime of only ~ 2.2 ns (1.1 ns), which is considerably shortened due to intermolecular interactions that introduce efficient non-radiative decay pathways.⁵

3.2 Dark current and Dc Photocurrent

Figure 5 shows dark current (a) and photocurrent (b) measured under 532 nm and 355 nm photoexcitation of pristine t-bu BTBTB and guest-host ADT-TES-F/t-bu BTBTB films at 2 mol %, 0.2 mol %, and 0.02 mol % ADT-TES-F concentrations. The dark current significantly improved as the ADT-TES-F concentration increased due to improved hole injection from Au electrodes (consistent with the relative HOMO energies of the ADT-TES-F (5.35 eV) and t-bu BTBTB (5.75 eV) with respect to the work function of Au at 5.1 eV) and due to charge transport via ADT-TES-F molecules. At 532 nm excitation, no photocurrent was observed in pristine t-bu BTBTB, which is expected since t-bu BTBTB does not absorb at 532 nm. Upon addition of ADT-TES-F to t-bu BTBTB, the photocurrent appeared and increased dramatically as the ADT-TES-F concentration increased from 0.02 to 2 mol %. At 2 mol %, at light intensity of ~ 15 mW/cm², the photocurrent was about two orders of magnitude higher than the dark current. It is interesting to note that at 532 nm, the photocurrent would be solely due to photoexcitation of ADT-TES-F and that charge transport must rely on the network of ADT-TES-F molecules. In particular, it cannot be due to charge propagation in the t-bu BTBTB, since it is energetically unfavorable for a charge carrier to transfer from an ADT-TES-F to a t-bu BTBTB molecule. At our doping concentrations of 0.02-2 mol %, the estimated average distance between the ADT-TES-F guest molecules varies from ~ 145 Å (at 0.02 mol %) to ~ 30 Å (at 2 mol %), which are significantly larger than those typically used in molecularly doped polymers with charge transport via guest molecules.¹⁵ This suggests that the wave function of the guest molecule (i.e. of ADT-TES-F) has a much larger extent as compared to that of molecular dopants utilized in typical polymeric systems.^{15,16} Both dark and cw photocurrents obtained at our highest ADT-TES-F concentration of 2 mol % were, however, at least two orders of magnitude lower than those measured in pristine ADT-TES-F films.⁵

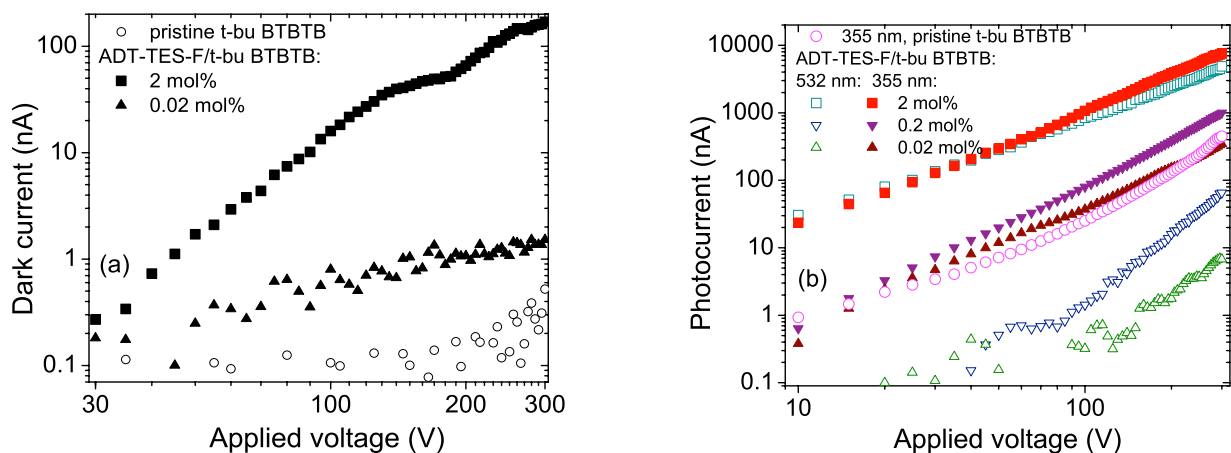


Figure 5. (a) Dark current of films of pristine t-bu BTBTB and in ADT-TES-F/t-bu BTBTB films at 2 mol % and 0.02 mol % ADT-TES-F concentration. (b) Photocurrent in ADT-TES-F/t-bu BTBTB films at three ADT-TES-F concentrations under 532 nm and 355 nm excitation. Also shown is photocurrent measured in pristine t-bu BTBTB film at 355 nm excitation.

At 355 nm excitation, several processes occur in the composite films, such as direct excitation of both t-bu BTBTB host and ADT-TES-F guest, as well as the energy transfer from t-bu BTBTB to ADT-TES-F. Significant photocurrent was observed in all samples, exhibiting a considerable increase as the concentration of ADT-TES-F increased, due to the establishment of a charge transport pathway via ADT-TES-F molecules (in addition to that via t-bu BTBTB molecules). Interestingly, at 2 mol % concentration of ADT-TES-F in t-bu BTBTB, the photocurrent at 355 nm was comparable to that at 532 nm, which suggests that at 355 nm excitation, a significant portion of the excitation is transferred to ADT-TES-F molecules via energy transfer from t-bu BTBTB (Fig. 3), followed by charge transport similar to that initiated by 532 nm excitation.

3.3 Photobleaching Quantum Yield

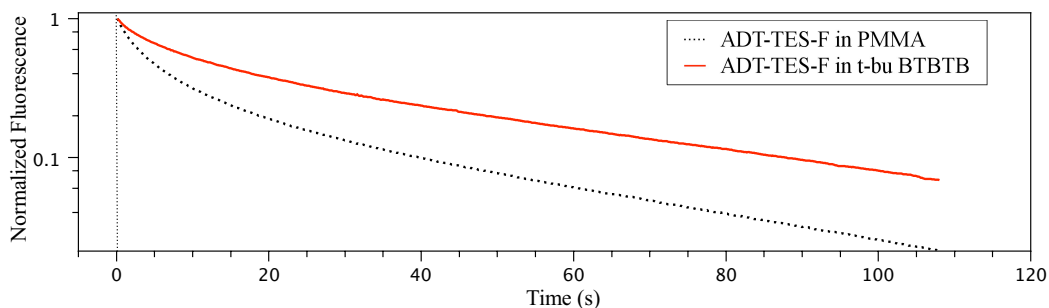


Figure 6. Normalized fluorescence vs time for ADT-TES-F at concentrations of 0.2 mol % in PMMA and t-bu BTBTB films under widefield 532 nm cw excitation at 200 W/cm².

One of the most important molecular characteristics of a SMFS fluorophore is its photostability, characterized by a photobleaching quantum yield Φ_b , which is the probability for the molecule to photobleach upon absorption of a photon. Φ_b of a fluorophore can be calculated from PL decays under continuous illumination such as those shown in Fig. 6 and generally depends on the environment surrounding the fluorophores. In order to verify our technique, we measured Φ_b of DCDHF-N-6 in PMMA to be 4.2×10^{-7} which is comparable to the value calculated from literature of 3.7×10^{-7} .¹⁰ From the data in Fig. 6 and our estimate of ADT-TES-F absorption cross-section

of $\sigma_{532} = 1.2 \times 10^{-16} \text{ cm}^2$ at 532 nm, Φ_b for ADT-TES-F in PMMA and in t-bu BTBTB were estimated to be 1.1×10^{-6} and 4.7×10^{-7} , respectively. These values are significantly lower (i.e. better) than, for example, those measured in various standard fluorophores used in SMFS (such as R6G, Texas Red, and Fluorescein) in aqueous environments and are comparable to DCDHF-N-6 in aqueous gelatin.¹⁰ Note that the polycrystalline t-bu BTBTB environment increases the photostability of ADT-TES-F, as compared to the amorphous polymer (PMMA) environment.

Another important characteristic of a SMFS fluorophore is the total number of photons (N_{tot}) it emits before photobleaching. Demonstrably good single molecule fluorophores have N_{tot} values on the order of 10^6 .¹⁷ Based on an estimate of the PL quantum yield of ADT-TES-F in PMMA ($\sim 87\%$) and the value of Φ_b , we calculate N_{tot} to be 7.6×10^5 using Eq. 2.

3.4 ADT-TES-F as a Single-Molecule Fluorophore

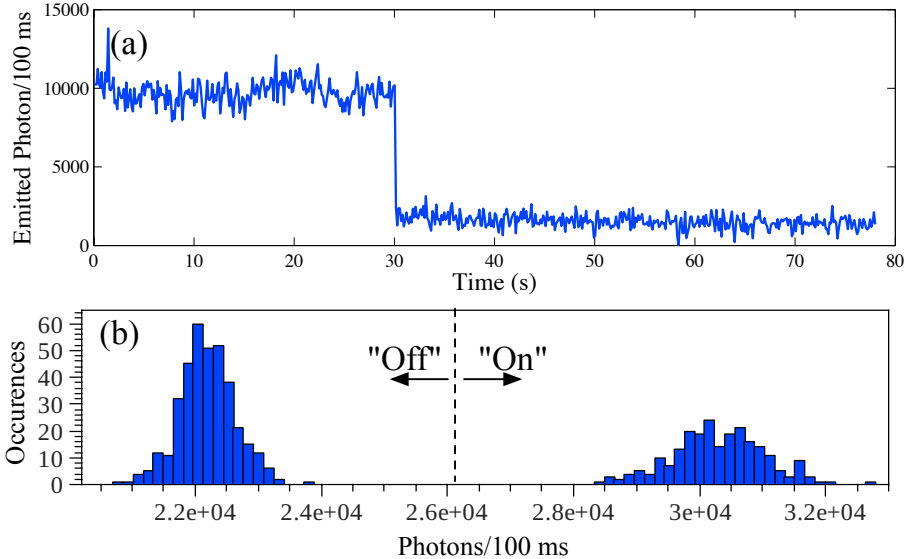


Figure 7. (a) A fluorescence trajectory for a single ADT-TES-F molecule showing single-step photobleaching, characteristic of a single molecule. (b) Fluorescence intensity histogram showing distinct two level system for the same molecule whose trajectory is shown in (a).

Single molecule data for ADT-TES-F in PMMA shown in Figure 7 was collected at 650 W/cm^2 cw 532 nm excitation. Over 100 ADT-TES-F molecules were imaged and analyzed. One such fluorescence trajectory, which shows single step photobleaching characteristic of a single molecule, is shown in Figure 7 along with the intensity histogram showing distinct "on" and "off" states. Approximately 10% of the analyzed ADT-TES-F molecules showed significant blinking behavior. From trajectories of all single molecules of ADT-TES-F which were analyzed, N_{tot} was determined by integrating individual single molecule fluorescence time traces, the average of which was found to be 6.2×10^5 which compares favorably with the value 7.6×10^5 obtained from bulk measurements above. Of the 10% which showed blinking behavior, the average "on" time τ_{on} showed relatively little fluorophore-to-fluorophore variation. This property could make ADT-TES-F molecules a useful nanoprobe of charge transfer in films at the microscopic level, as variation in τ_{on} may be attributable to charge transfer processes and can be analyzed to obtain charge transfer rates.¹¹ Furthermore, our preliminary tests suggest that ADT-TES-F can be imaged at the single molecule level in a host matrix of t-bu BTBTB making this system promising for studying charge transfer at the molecular level.

4. CONCLUSIONS

In summary, we explored optical, PL, and (photo)conductive properties of novel ADT-TES-F/t-bu BTBTB composites. Energy transfer from t-bu BTBTB to ADT-TES-F molecules was observed at 355 nm photoexci-

tation. At both 355 nm and 532 nm excitation, dc photocurrent dramatically improved as the concentration of ADT-TES-F increased from 0.02 mol % to 2 mol % moles per mole of t-bu BTBTB, which suggests that already at 0.2 mol % ADT-TES-F concentration, charge transport can proceed via ADT-TES-F molecules and at 2 mol % ADT-TES-F concentration, transport via ADT-TES-F molecules dominates the photocurrent in ADT-TES-F/t-bu BTBTB composites.

ADT-TES-F molecules also exhibit high PL quantum yields, low photobleaching quantum yields, and good stability with respect to blinking in solid-state environments, which makes them attractive for SMFS. Our ability to image single molecules of ADT-TES-F in t-bu BTBTB offers a promising venue to explore charge transfer processes on a molecular level in small-molecular weight organic semiconductors.

5. ACKNOWLEDGEMENTS

We thank Prof. R. J. Twieg for supplying DCDHF-N-6. This work was supported in part by the Office of Naval Research (grant #N00014-07-1-0457 via ONAMI Nanometrology and Nanoelectronics Initiative), and National Science Foundation via CAREER program (DMR-0748671).

REFERENCES

- [1] Forrest, S. R., "The path to ubiquitous and low-cost organic electronic appliances on plastic," *Nature* **428**, 911 (2004).
- [2] Anthony, J. E., "Functionalized acenes and heteroacenes for organic electronics," *Chem. Rev.* **106**, 5028–5048 (2006).
- [3] Subramanian, S., Park, S. K., Parkin, S. R., Podzorov, V., Jackson, T. N., and Anthony, J. E., "Chromophore fluorination enhances crystallization and stability of soluble anthradithiophene semiconductors," *J. Am. Chem. Soc.* **130**, 2706 (2008).
- [4] Park, S. K., Mourey, D. A., Subramanian, S., Anthony, J. E., and Jackson, T. N., "High-mobility spin-cast organic thin film transistors," *Appl. Phys. Lett.* **93**, 043301 (2008).
- [5] Platt, A. D., Day, J., Subramanian, S., Anthony, J. E., and Ostroverkhova, O., "Optical, fluorescent, and (photo)conductive properties of high-performance functionalized pentacene and anthradithiophene derivatives," *J. Phys. Chem. C* **113**(31), 14006–14014 (2009).
- [6] Day, J., Subramanian, S., Anthony, J. E., Lu, Z., Twieg, R. J., and Ostroverkhova, O., "Photoconductivity in organic thin films: From picoseconds to seconds after excitation," *J. Appl. Phys.* **103**, 123715 (2008).
- [7] Day, J., Platt, A. D., Ostroverkhova, O., Subramanian, S., and Anthony, J. E., "Organic semiconductor composites: influence of additives on the transient photocurrent," *Appl. Phys. Lett.* **94**, 013306 (2009).
- [8] Platt, A. D., Shepherd, W. E. B., Anthony, J. E., and Ostroverkhova, O., "Photophysical and photoconductive properties of organic semiconductor composites," *SPIE Linear and Nonlinear Optics of Organic Materials IX* **7413**(1), 74130S (2009).
- [9] Ostroverkhova, O., Platt, A. D., Shepherd, W. E. B., Day, J., and Anthony, J. E., "Optical and electronic properties of functionalized pentacene and anthradithiophene derivatives," *SPIE Linear and Nonlinear Optics of Organic Materials IX* **7413**(1), 74130A (2009).
- [10] Lord, S. J., Lu, Z., Wang, H., Willets, K. A., Schuck, P. J., Lee, H.-I. D., Nishimura, S. Y., Twieg, R. J., and Moerner, W. E., "Photophysical properties of acene DCDHF fluorophores: Long-wavelength single-molecule emitters designed for cellular imaging," *J. Phys. Chem. A* **111**, 8934–8941 (2007).
- [11] Holman, M., Liu, R., and Adams, D., "Single-molecule spectroscopy of interfacial electron transfer," *J. Am. Chem. Soc.* **125**(41), 12649–12654 (2003).
- [12] Hoogenboom, J., Hernando, J., and van Dijk, E., "Power-law blinking in the fluorescence of single organic molecules," *Chem. Phys. Chem.* **8**, 823–833 (2007).
- [13] Ostroverkhova, O., Shcherbina, S., Cooke, D. G., Egerton, R. F., Hegmann, F. A., Tykwinski, R. R., Parkin, S. R., and Anthony, J. E., "Optical and transient photoconductive properties of pentacene and functionalized pentacene thin films: Dependence on film morphology," *J. Appl. Phys.* **98**, 033701 (2005).

- [14] Fujii, M., Yoshida, M., Kanzawa, Y., and Hayashi, S., “1.54 μm photoluminescence of Er^{3+} doped into SiO_2 films containing Si nanocrystals: Evidence for energy transfer from Si nanocrystals to Er^{3+} ,” *Appl. Phys. Lett.* **71**(9), 1198–1200 (1997).
- [15] Schein, L. B., Weiss, D. S., and Tyutnev, A., “The charge carrier mobility’s activation energies and pre-factor dependence on dopant concentration in molecularly doped polymers,” *Chemical Physics* **365**(3), 101–108 (2009).
- [16] Coehoorn, R., “Hopping mobility of charge carriers in disordered organic host-guest systems: Dependence on the charge-carrier concentration,” *Phys. Rev. B* **75**(15), 155203 (2007).
- [17] Willets, K. A., Ostroverkhova, O., He, M., Twieg, R. J., and Moerner, W. E., “Novel fluorophores for single-molecule imaging,” *J. Am. Chem. Soc.* **125**(5), 1174–1175 (2003).